

Prospects for the measurement of ice cloud particle shape and orientation with elliptically polarized radar signals

S. Y. Matrosov¹

Wave Propagation Laboratory, National Oceanic and Atmospheric Administration, Boulder, Colorado

(Received July 23, 1990; revised March 22, 1991; accepted March 22, 1991.)

A method to estimate cloud particle orientation and shape parameters using a polarization diversity radar is presented. The method is demonstrated for low-reflectivity ice clouds containing crystals that are modeled as prolate and oblate spheroids. The parameters to be estimated are the particle mean canting angle and the axis ratio in the incident wave polarization plane. The scattering matrix concept is used to obtain a relationship between two orthogonally polarized received powers and the parameters of interest. It is shown that the use of an elliptically polarized radar signal diminishes the expected difference between received powers in the two receiving polarization channels. This makes polarization studies of ice clouds with relatively low reflectivities possible; these clouds often are “invisible” in one of the receiving channels when conventional linear or circular polarization is used. An estimation of errors in the retrieved mean canting angle value caused by the spread in particle orientation is also given.

1. INTRODUCTION

Knowledge of cloud particle shapes and orientation is important for many practical and theoretical investigations in atmospheric physics, remote sensing, climatology, weather modification, and radio communication; however, direct measurements of these cloud characteristics from aircraft are difficult and expensive. Polarization diversity radars provide the possibility for indirect measurements of particle shapes and orientation [Bringi and Hendry, 1990].

Usually, meteorological polarization diversity radars transmit either a linearly or a circularly polarized electromagnetic wave and use two receivers: one for copolar and the other for cross-polar components of reflected signals. Linear or circular depolarization ratios (LDR and CDR), which represent the ratios of measured power in the two polarization receiving channels, are informative polarization parameters. If linear rather than logarithmic receivers are used, a correlation coefficient between the two circularly polarized components of reflected signals can be used to estimate the intrinsic degree of scatterer orientation and the scatterer

mean canting angle [McCormick and Hendry, 1975]. However, determining this angle requires measuring the phase difference between the two polarization amplitudes, which is not always feasible.

Ice clouds are of main interest when studying particle shapes and orientation because liquid water drops in nonprecipitating clouds are nearly spherical. However, clouds containing mostly ice particles (for example, cirrus and stratus clouds) are often optically thin and produce low radar reflectivities. Sometimes they are “invisible” in the orthogonal receiver channel even when using radars that operate in the millimeter wavelength region, which are inherently more sensitive to small particles than are longer wavelength radars. Received power measured in the orthogonal receiving channel can be 15–35 dB lower than power in the main channel when CDR or LDR measurements are carried out. The orthogonal signal, for example, for cirrus clouds, can be weaker than –30 to –35 dBZ [Kropfli *et al.*, 1990], which is usually below the “detectability” threshold for most meteorological radars.

Alternatively, one can obtain differential reflectivity (Z_{DR}) data that represent the ratio of received power of copolarized signals in two orthogonal linear polarizations. These signals may have comparable magnitudes, but Z_{DR} data display combined effects of scatterer shape and orientation in the directions fixed by the chosen polarization basis.

¹ On leave from the Main Geophysical Observatory, Leningrad, USSR.

The separate effects of shape and orientation cannot be distinguished using only Z_{DR} measurements.

The problem of optimal elliptical polarization for studying fluctuating radar targets has been discussed by *McCormick and Hendry* [1985] and *Mel'nik and Ryzhkov* [1985]. Optimal polarization states depend on scatterer orientation and shape and produce the minimum return signal in one of the two receiving channels. Thus these are polarization states in which maxima of the absolute values of the depolarization ratios are achieved, and they are inappropriate for studying low-reflectivity ice clouds.

In this paper we explore the possibility of estimating particle axial ratios and canting angles in the incident wave polarization plane from measurements with elliptically polarized radar signals. We show that the proper choice of elliptical polarization will increase the signal level in the orthogonal channel relative to the main channel and that the use of two different states of elliptical polarization allows one to distinguish between the effects of particle shape and those of orientation.

2. THEORY

In many optical systems, and in some polarization diversity radars, a rotatable quarter-wave plate is used to change the polarization of transmitted signals [*Kanareikin et al.*, 1990]. This is the technique that is considered here, although the proposed polarization state changes can be achieved by other technologies. Such a plate is being implemented in the Wave Propagation Laboratory (WPL) Ka-band radar [*Kropfli et al.*, 1990]. This radar is designed for application in cloud microphysics and climate research programs.

The quarter-wave plate introduces a 90° phase shift between two orthogonal linearly polarized components of the signal that coincide with the plate optical axes. It can be assumed without losing generality that the radar signal incident on the plate is horizontally polarized. The normalized Stokes vector of a horizontally polarized electromagnetic wave is

$$Q_h = (1, 1, 0, 0)^* \quad (1)$$

where the asterisk is the transposition sign.

If Q is the Stokes vector of the received electromagnetic wave after passing the quarter-wave plate

in the reverse direction, then normalized powers in the copolar (co) and cross-polar (cr) receiving channels are

$$P_{co} = (Q, Q_h) \quad (2)$$

$$P_{cr} = (Q, Q_v)$$

where parentheses denote the scalar multiplication of vectors and Q_v is the Stokes vector of a vertically polarized electromagnetic wave given by

$$Q_v = (1, -1, 0, 0)^* \quad (3)$$

The Mueller matrix of a quarter-wave plate [*Bohren and Huffman*, 1983] is

$$L(\beta) = \begin{vmatrix} 1 & 0 & 0 & 0 \\ 0 & \cos^2 2\beta & \sin 2\beta \cos 2\beta & -\sin 2\beta \\ 0 & \sin 2\beta \cos 2\beta & \sin^2 2\beta & \cos 2\beta \\ 0 & \sin 2\beta & -\cos 2\beta & 0 \end{vmatrix} \quad (4)$$

where β is the angle between the horizontal and one of the two optical axes of the plate, i.e., the axis for which phase increases with range at a faster rate.

The Stokes vector Q of the received signal can be obtained as a result of the following matrix transformation:

$$Q = L(-\beta) \cdot M \cdot L(\beta) \cdot Q_h \quad (5)$$

where M is the Mueller matrix of meteorological targets in the radar-illuminated volume.

Rotating the quarter-wave plate changes the relationship between reflected signals in the copolar and cross-polar channels. Depending on the value of angle β , either the copolar or the cross-polar channel becomes the main channel, which is defined as the channel in which the polarization component of received signals is stronger than in the orthogonal channel. It can easily be shown that for most meteorological targets the main channel is the copolar channel for linearly polarized radar signals ($\beta = 0^\circ$) and it is the cross-polar channel for circularly polarized signals ($\beta = 45^\circ$). If scatterers are perfect spheres, the two polarization components are equal for elliptically polarized radar signals with $\beta = 22.5^\circ$.

According to *Magono and Lee* [1966], the most frequent forms of crystals in nonprecipitating ice clouds are plates, bullets, columns, and needles, which are modeled here as oblate and prolate spheroids. This simple model was assumed because the

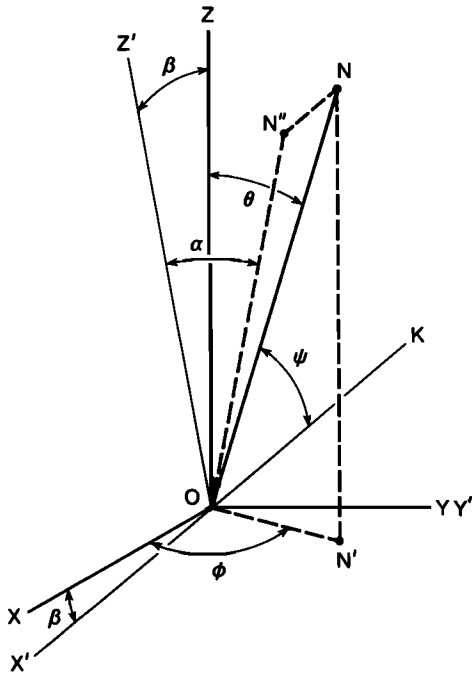


Fig. 1. Geometry of scattering.

relatively large uncertainty in our knowledge of crystal shapes makes more complicated models superfluous.

The Mueller matrix of scatterers can be obtained from the four elements of the amplitude backscattering matrix S , which gives the relationship between the electric field components of scattered (s) and incident (i) electromagnetic waves [Van de Hulst, 1983]. In the linear basis of horizontal (h) and vertical (v) polarizations for one spheroidal particle,

$$\begin{bmatrix} E_h \\ E_v \end{bmatrix}_{(s)} \approx \frac{e^{ikr}}{-ikr} \begin{bmatrix} s_{hh} \cos^2 \alpha - s_{vv} \sin^2 \alpha & -(s_{vv} + s_{hh}) \sin 2\alpha/2 \\ (s_{hh} + s_{vv}) \sin 2\alpha/2 & s_{vv} \cos^2 \alpha - s_{hh} \sin^2 \alpha \end{bmatrix} \begin{bmatrix} E_h \\ E_v \end{bmatrix}_{(i)} \quad (6)$$

In (6), α is the canting angle in the incident wave polarization plane ($Z'OY'$ in Figure 1), i.e., the angle between the projection (ON' in Figure 1) of the particle symmetry axis (ON in Figure 1) onto

the wave polarization plane and the direction of the vertical polarization (OZ' in Figure 1). Holt [1984] showed that scattering amplitudes s_{hh} and s_{vv} can be expressed in terms of the scattering amplitudes along the particle symmetry axis (s_h) and the axis that is perpendicular to it (s_v). Taking into account the inversion of the original coordinate system after a backscattering event, for a small particle,

$$\begin{aligned} s_{hh} &= s_h \\ s_{vv} &= -s_h \cos^2 \psi + s_v \sin^2 \psi \end{aligned} \quad (7)$$

where ψ is the angle between the particle symmetry axis and the incident wave propagation.

Figure 1 shows the relations of α and ψ with respect to the scatterer orientation. Angles θ and ϕ give the direction of the particle symmetry axis (ON) in the spherical coordinate system. Angle β is the radar elevation angle, and OK shows the direction of the incident wave propagation. Relationships between trigonometrical functions of these angles can be found in the work by Holt [1984].

For small ice particles the real part of the scattering amplitudes is much less than the imaginary part [$|\text{Im}(s_{h(v)})/\text{Re}(s_{h(v)})| \sim 10^2 - 10^3$], and therefore these amplitudes can be treated as pure imaginary. Thus it can be defined that

$$A = -s_{hh}/s_{vv} \quad (8)$$

where ratio A is a real factor (A is greater than 1 for oblate particles and A less than 1 for prolate ones). When the particle's symmetry axis is parallel to the unit vector of vertical polarization of the incident wave, A represents the square root of the differential reflectivity.

Ratio A is related to B , the ratio of the particle's minor-to-major dimensions in the incident wave polarization plane. If $\psi = 90^\circ$, B is equal to the ratio of the minor axis to the major axis of the spheroidal particle. Figure 2 depicts A as a function of B for two different complex refractive indices of ice $m = 1.78 + i0.0007$ and $m = 1.60 + i0.0006$, corresponding to the bulk densities of 0.9 g cm^{-3} and 0.6 g cm^{-3} [Rozenberg, 1972], which represent the approximate limits of ice crystal density variation [Pruppacher and Klett, 1978]. Analogous information on the linear depolarization properties of oblate and prolate spheroids can be found in the work by Atlas et al. [1953]. The results presented here were obtained using the Rayleigh approximation, which

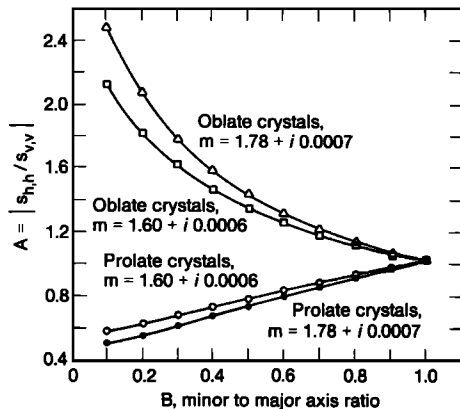


Fig. 2. Scattering amplitude ratio as a function of minor-to-major axis ratio of particles for different complex refractive indices of ice.

is valid for ice particles with major dimensions of less than 1 mm at a frequency of 30 GHz [Yeh *et al.*, 1982]. According to Pruppacher and Klett [1978], particle sizes in nonprecipitating ice clouds usually do not exceed this value, so the Rayleigh approximation is generally valid for such clouds up to the Ka-band.

The backscattering matrix in (6) can be rewritten in terms of A and α as

$$\mathbf{S} = s_0 \begin{bmatrix} A \cos^2 \alpha + \sin^2 \alpha & (1 - A) \sin \alpha \cos \alpha \\ (A - 1) \sin \alpha \cos \alpha & -\cos^2 \alpha - A \sin^2 \alpha \end{bmatrix} \quad (9)$$

where s_0 is an imaginary factor that can be omitted when relative polarization parameters are considered. Using the relationships between the amplitude backscattering matrix \mathbf{S} and the Mueller matrix \mathbf{M} [Bohren and Huffman, 1983], one can obtain for normalized elements of \mathbf{M} ,

$$m_{11} = 0.5(A^2 + 1) \quad (10a)$$

$$m_{12} = m_{21} = 0.5 \cos 2\alpha (A^2 - 1) \quad (10b)$$

$$m_{13} = -m_{31} = 0.5 \sin 2\alpha (1 - A^2) \quad (10c)$$

$$m_{22} = 0.5[\cos^2 2\alpha (A - 1)^2 + 2A] \quad (10d)$$

$$m_{23} = -m_{32} = -0.5 \sin 2\alpha \cos 2\alpha (A - 1)^2 \quad (10e)$$

$$m_{33} = -A \cos^2 2\alpha - 0.5 \sin^2 2\alpha (1 + A^2) \quad (10f)$$

$$m_{44} = -A \quad (10g)$$

$$m_{14} = m_{24} = m_{34} = m_{41} = m_{42} = m_{43} = 0. \quad (10h)$$

We assume further that the Mueller matrix elements of an ensemble of scatterers in the radar-illuminated volume are also given by (10), where α is the weighted mean canting angle and A is the weighted mean ratio of the particles' scattering amplitudes in the incident wave polarization plane. The errors caused by such an assumption are considered in section 3.2.

It can be seen from (1)–(3) that only the first two components of the Stokes vector \mathbf{Q} are important for measuring power in the main and orthogonal channels. These components can be obtained from (5):

$$q_1(\beta) = m_{11} + m_{12} \cos^2 2\beta + m_{13} \sin 2\beta \cos 2\beta, \quad (11a)$$

$$q_2(\beta) = m_{21} \cos^2 2\beta + m_{22} \cos^4 2\beta + 2m_{23} \sin 2\beta \cos^3 2\beta - m_{31} \sin 2\beta \cos 2\beta - m_{33} \sin^2 2\beta \cos^2 2\beta + m_{44} \sin^2 2\beta. \quad (11b)$$

Then normalized powers of the received signals in the copolar and cross-polar channels are

$$P_{co}(\beta) = q_1(\beta) + q_2(\beta) \quad (12a)$$

$$P_{cr}(\beta) = q_1(\beta) - q_2(\beta) \quad (12b)$$

The conventional radar polarization parameters are obtained for linearly ($\beta = 0^\circ$ or $\beta = 90^\circ$) or for circularly ($\beta = 45^\circ$) polarized incident waves

$$\text{LDR} = 10 \log_{10}[P_{cr}(0^\circ)/P_{co}(0^\circ)] \quad (13a)$$

$$\text{CDR} = 10 \log_{10}[P_{co}(45^\circ)/P_{cr}(45^\circ)] \quad (13b)$$

As mentioned before, received signals in the copolar and cross-polar channels can differ by as much as 15–35 dB when linear or circular polarization is used, and therefore the received power in the orthogonal channel may be too low to detect. One solution to this problem is to use elliptically polarized incident waves. Rotating the quarter-wave plate to an angle between 0° and $\pm 45^\circ$ produces an elliptically polarized transmitted wave with the ellipticity angle equal to the azimuth angle of the polarization ellipse. The normalized Stokes vector of such a wave is.

$$\mathbf{Q}_i = (1, \cos^2 2\beta, \sin 2\beta \cos 2\beta, \sin 2\beta)^* \quad (14)$$

It can be seen from (11) and (12) that measurements at angles $\beta = 22.5^\circ$ and $\beta = -22.5^\circ$ can yield an estimate of several normalized Mueller matrix elements and their linear combinations:

$$m_{13} = 0.5(P_{co}^a + P_{cr}^a - P_{co}^b - P_{cr}^b) \quad (15a)$$

$$m_{12} + 2m_{11} = 0.5(P_{co}^a + P_{cr}^a + P_{co}^b + P_{cr}^b) \quad (15b)$$

$$m_{13} + m_{23} = 0.5(P_{co}^a + P_{cr}^b - P_{cr}^a - P_{co}^b) \quad (15c)$$

$$m_{12} + m_{44} + 0.5(m_{22} - m_{33}) = 0.5(P_{co}^a + P_{co}^b - P_{cr}^a - P_{cr}^b) \quad (15d)$$

where superscripts *a* and *b* denote received power measurements at $\beta = 22.5^\circ$ and $\beta = -22.5^\circ$, respectively.

Further, taking into account the expressions for the Mueller matrix elements (10), the following system of equations for *A* and $\cos \alpha$ can be obtained

$$\begin{aligned} (A^2 - 1) \cos 2\alpha / (A + 1)^2 &= 2(P_{cr}^b - P_{cr}^a) / (P_{co}^a + P_{cr}^a - P_{co}^b \\ &- P_{cr}^b) \equiv G_1 \\ [\cos 2\alpha(A^2 - 1) + 0.5(A - 1)^2] / [2A^2 + \cos 2\alpha(A^2 - 1) \\ &+ 2] &= (P_{co}^a + P_{co}^b - P_{cr}^a - P_{cr}^b) / (P_{co}^a + P_{co}^b + P_{cr}^a \\ &+ P_{cr}^b) \equiv G_2 \end{aligned} \quad (16)$$

The right sides of these equations contain ratios of linear combinations of four measurable powers in the two channels and at the two positions of the quarter-wave plate. Such relative elliptical polarization measurements will yield values of *A* and α . Solving the system of equations gives the following quadratic equation for *A*

$$\begin{aligned} A^2(G_1G_2 + 2G_2 - G_1 - 0.5) + A(2G_1G_2 - 2G_1 + 1) \\ + (G_1G_2 + 2G_2 - G_1 - 0.5) &= 0. \end{aligned} \quad (17)$$

Equation (17) yields two values for *A*. One solution corresponds to prolate particles and the other to oblate ones. It is also true that $A_1 \cdot A_2 = 1$. Corresponding values of $\cos \alpha$ are

$$\cos 2\alpha_1 = G_1(A_1 + 1)^2 / (A_1^2 - 1) \quad (18a)$$

$$\cos 2\alpha_1 = -\cos 2\alpha_2 \quad (18b)$$

Such an ambiguity exists for Rayleigh scatterers because prolate particles with their symmetry axes

inclined at an angle of α and oblate ones inclined at an angle of $90^\circ + \alpha$ produce an identical backward (and forward) scattered electromagnetic field if both types of the particles have the same major-to-minor scattering amplitude ratio ($A_1 = 1/A_2$). There is no way to distinguish between prolate and oblate scatterers when measurements are carried out at a fixed elevation angle.

Knowing *A*, one can estimate the average minor-to-major axis ratio of scatterers in the incident wave polarization plane from Figure 2. This value will give an estimate of the minor-to-major particle axis ratio if $\psi = 90^\circ$. Otherwise, from *A* we can obtain information about the particle minor-to-major dimension ratio in the incident wave polarization plane. It should be mentioned, however, that there are no other methods to obtain estimates of the latter ratio from radar polarization measurements at a fixed viewing geometry. It can be seen also from Figure 2 that uncertainty in the particle complex refractive index can cause errors in the estimated values of axis ratio. These errors will be small for ice clouds in the upper troposphere but they can be relatively large when studying aggregates. In the latter case some a priori data or supporting measurements of hydrometeor density are needed.

3. DISCUSSION

Calculations were performed to illustrate the potential for obtaining cloud particle shape and orientation characteristics using elliptically polarized radar signals. Because oblate and prolate scatterers cannot be distinguished from each other by measurements at a fixed radar elevation angle, the illustrations that follow are presented for different values of scattering amplitude ratio A_0 defined as

$$A_0 = \max(|s_{hh}|, |s_{vv}|) / \min(|s_{hh}|, |s_{vv}|) \quad (19)$$

Data shown for a canting angle of α correspond to either prolates with the canting angle α or oblates with the canting angle $90^\circ + \alpha$. This angle can also be considered the major axis inclination angle of the particle from the direction of the vertical polarization in the incident wave polarization plane.

3.1. Received power dependence on particle orientation

Figure 3 depicts characteristics of received powers in both channels at different quarter-wave plate

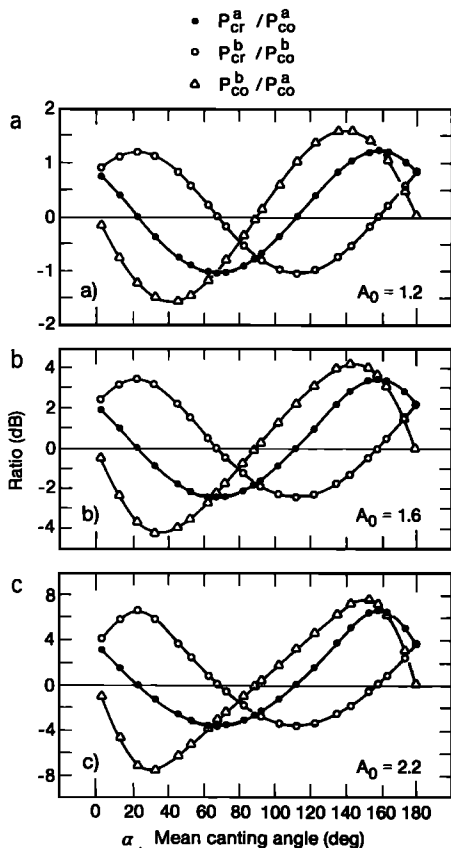


Fig. 3. Power ratios in copolar and cross-polar channels at different positions of a quarter-wave plate as a function of scatterer mean canting angles for different degrees of particle deformation; (a) $A_0 = 1.2$, (b) $A_0 = 1.6$, (c) $A_0 = 2.2$.

positions as a function of scatterer canting angle for depolarizations with various degrees of deformation. The depolarization ratios P_{cr}^a/P_{co}^a , P_{cr}^b/P_{co}^b , and the copolar ratio are presented for both positions of the quarter-wave plate ($\beta = 22.5^\circ$ and $\beta = -22.5^\circ$). These data show that values of received powers differ by less than 1.5 dB for slightly deformed particles with $A_0 = 1.2$ (which corresponds to mean minor-to-major particle axis ratio $B \approx 0.8$) and up to about 7 dB for particles with a relatively high degree of deformation ($A_0 = 2.2$, $B \approx 0.15-0.2$). Received signals in the copolar and cross-polar channels are equal when $\alpha = 22.5^\circ$ or $\alpha = 112.5^\circ$ (if $\beta = 22.5^\circ$) and $\alpha = 67.5^\circ$ or $\alpha = 157.5^\circ$ (if $\beta = -22.5^\circ$). The received power in the copolar channel is maximal when $\alpha = 67.5^\circ$ and $\alpha = 112.5^\circ$ for $\beta = 22.5^\circ$ and $\beta = -22.5^\circ$, respectively.

Figure 4 shows the received power on the sug-

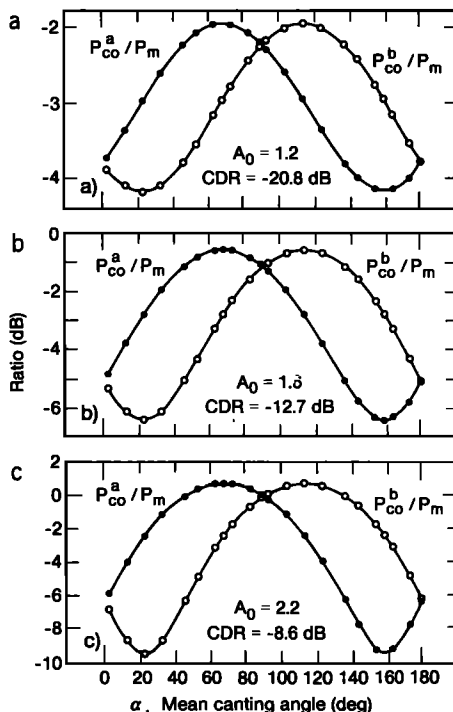


Fig. 4. Ratios of copolar channel power on the elliptical polarization to the main channel power on the circular polarization as a function of scatterer mean canting angle for different degrees of particle deformation; (a) $A_0 = 1.2$, (b) $A_0 = 1.6$, (c) $A_0 = 2.2$.

gested elliptical polarizations compared with received power on the circular polarization. The curves for the three particle deformations are very similar in shape but differ in magnitude. The ratios shown are P_{co}^a/P_m and P_{co}^b/P_m , where P_m is the backscattered radar signal received in the main channel when measurements are made on the circular polarization ($P_m = P_{cr}(\beta = 45^\circ)$). The ratios of P_{cr}^a/P_m and P_{cr}^b/P_m are not shown here because their magnitudes are within the limits of variability of P_{co}^a/P_m and P_{co}^b/P_m .

For the least deformed particles ($A_0 = 1.2$), measured signals in both receiver channels for $\beta = \pm 22.5^\circ$ are much stronger than those in the orthogonal channel [$P_{co}(\beta = 45^\circ)$] when circular polarization measurements are performed. The corresponding CDR value in this case is -20.8 dB, regardless of the scatterer canting angle. LDR strongly depends on particle orientation and is almost always less than CDR.

The above comments are also valid for moder-

ately deformed particles ($A_0 = 1.6$), though in this case the CDR value is higher (-12.7 dB). For scatterers with a relatively high degree of deformation ($A_0 = 2.2$), reflected signals of interest vary approximately over the same range of values as signals in the main and orthogonal channels for the circular polarization. The corresponding value of CDR for these scatterers is -8.6 dB.

From the above considerations we conclude that for the measurements employing elliptical polarization the expected power values in the copolar and cross-polar receiving channels do not differ by more than 8–10 dB. These values as a rule exceed the power in the orthogonal channel when CDR or LDR measurements are made.

This last statement can be confirmed by the following considerations. During the summer season of 1990 the WPL Ka-band radar [Kropfli *et al.*, 1990], prior to installation of the new polarization antenna, was used to observe cirrus clouds. No depolarization measurements were made during these observations. Typical radar echoes from this class of clouds were about -20 dBZ in the main circular channel. It means that radar echoes in the orthogonal circular channel would be about -41 dBZ for slightly deformed particles (Figure 4a), -33 dBZ for moderately deformed particles (Figure 4b) and -29 dBZ for particles with relatively high degree of deformation (Figure 4c). A simple analysis shows that the radar reflectivity in the copolar channel on the linear polarization would be in the regions of approximately $-19 \sim -21$ dBZ (case a), $-18 \sim -22.5$ dBZ (case b), and $-17 \sim -24$ dBZ (case c), depending on the particle canting angle. Reflectivities in the cross-polar linear channel are less than those in the orthogonal channel on the circular polarization. Reflectivities on the proposed elliptical polarizations in both copolar and cross-polar channels vary between $-22 \sim -24.5$ dBZ, $-21 \sim -27$ dBZ, and $-19 \sim -29$ dBZ for the three cases discussed.

A new antenna being prepared for the WPL Ka-band radar will allow us to detect backscattered signals from cirrus clouds with the polarization cancellation ratio of better than -30 dB. The radar is able to detect -31 dBZ signals at a distance of 10 km. Thus the circular polarization technique can be applied to typical cirrus clouds only if scatterers are highly deformed and only for near-zenith-looking geometry because such clouds are usually observed at altitudes of 8–11 km. Using the proposed ellipti-

cal polarizations may provide an opportunity to study less deformed particles and possibly to apply tilt geometry.

These results also indicate that reflectivities on the two copolar linear polarizations (horizontal and vertical) are also within the acceptable limits for measurements. However, as stated above, differential reflectivity measurements do not allow one to distinguish between the effects of shape and orientation, i.e., to obtain simultaneously estimates of both α and A .

One can see from the above results that the dynamic range of elliptical reflectivities is rather small, approximately 2.5 dB for slightly deformed particles. However, with a measurement accuracy of about 0.5 dB, it might be possible to obtain scatterer shape and orientation information in those situations where conventional linear or circular polarization techniques are not helpful.

A potential source of errors in the proposed technique is the effect of propagation of the signal through the medium between the radar and the sample volume. Propagation effects in the ice crystal medium occur primarily because of the differential phase shift; differential attenuation is negligibly small. Analysis shows that the differential phase shift in the cirrus clouds is rather small. Model computations for hexagonal plates all orientated in the horizontal plane at a concentration providing ice mass content (IMC) 0.1 g m^{-3} and observed at low elevations give the magnitude of the differential phase shift of approximately $3^\circ/\text{km}$.

This estimation can be regarded as an upper limit because cirrus clouds are rather thin (typically less than 2 km) and usually have magnitudes of IMC less than that used in the estimation. In addition, hexagonal plates are among the most deformed particles found in the cirrus clouds [Pruppacher and Klett, 1978]. Such a differential phase shift can cause variations in the depolarization ratios of interest of about 0.25 dB, which is smaller than the usual measurements errors.

It should be mentioned, however, that the differential phase shift can be significant when studying more dense ice crystal media such as snowstorms, internal parts of anvils of heavy cumulus clouds, etc. In such cases, errors caused by differential phase shift could be unacceptably high, and special measures should be taken to minimize these effects. We also note that the existence and magnitude of propagation effects may be inferred from measure-

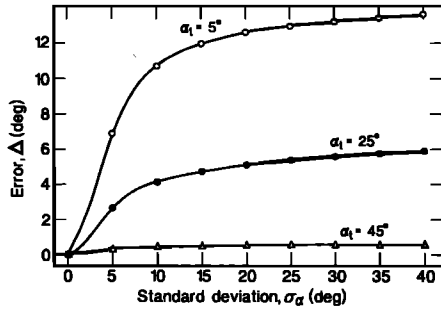


Fig. 5. Dependence of mean canting angle retrieval error on standard deviation of this angle.

ments of the complex ratio $\rho(45^\circ)/P_{cr}(45^\circ)$ [McCormick and Hendry, 1979] in different radar resolution cells. Here $\rho(45^\circ)$ is the correlation coefficient between the two orthogonal components of the received signal in the circular basis and $P_{cr}(45^\circ)$ was denoted above.

3.2. Influence of spread in canting angle distribution

All previous considerations assumed that scatterers in the illuminated volume are aligned. In reality, some spread around the mean canting angle can be expected. In this case the measured (retrieved) canting angle α_m would differ from the true α_t because of the nonlinearity of the equation system (16) and inaccuracy caused by assumption that equations (10) and (16), which are exact for an individual particle, are also valid for an ensemble of scatterers in terms of the weighted mean values of A and α . Such a difference will occur even in an ideal case in which measurements of received power are exact. So the error caused by the spread of canting angles can be considered an error that is intrinsic to the suggested technique. Figure 5 depicts this error, $\Delta = \alpha_t - \alpha_m$, as a function of the standard deviation of the canting angle distribution (σ_α) for different mean values of α_t . The error magnitudes were calculated assuming the Gaussian distribution for particle canting angles. Data are presented only for particles with relatively high degree of deformation ($A_0 = 2.2$).

The intrinsic errors can be greatest for particles with nearly horizontal orientation. These errors diminish when α approaches 45° and again rise when α decreases to 0° . The dependence of Δ on α_t is almost periodic, so data for only the canting angle region $0^\circ < \alpha_t < 45^\circ$ are shown in Figure 5. Similar

results were also obtained for particles with moderate and low degree of deformation. However, for these particles the errors discussed can be 10–20% higher than those shown in Figure 5.

It is obvious from the above considerations that estimating the scatterer degree of orientation is helpful in evaluating intrinsic errors of particle canting angles. One way to obtain such an estimation is to analyze the correlation coefficient between signal amplitudes in the copolar and cross-polar channels. McCormick and Hendry [1975] showed that a measure of the degree of particles' orientation could be determined from the correlation coefficient between the two circular polarization components of received signals.

Apparently, such an approach can also be applied when polarimetric measurements are made on the elliptical polarizations. Correlation coefficients for any polarization basis can be obtained from elements of the modified amplitude scattering matrix F , which is derived from the amplitude matrix S given by (9) as

$$F(\beta) = T(\beta) \cdot C \cdot T(-\beta) \cdot S \cdot T(-\beta) \cdot C \cdot T(\beta) \quad (20)$$

where C is the amplitude quarter-wave plate matrix and T is the rotation matrix [Born and Wolf, 1965]:

$$c = \begin{vmatrix} i & 0 \\ 0 & 1 \end{vmatrix} \quad (21a)$$

$$T(\beta) = \begin{vmatrix} \cos \beta & \sin \beta \\ -\sin \beta & \cos \beta \end{vmatrix} \quad (21b)$$

The product $T(-\beta) \cdot C \cdot T(\beta)$ in (18) describes the incident wave transformation by the quarter-wave plate, and the product $T(\beta) \cdot C \cdot T(-\beta)$ describes the transformation of the scattered wave. The generalized correlation coefficient is defined as

$$\rho(\beta) = \overline{|f_{1,1}|^2} \overline{|f_{2,1}|^2} / (\overline{|f_{2,1}|^2} \overline{|f_{1,1}|^2})^{1/2} \quad (22)$$

where $f_{1,1}$ and $f_{2,1}$ are elements of the matrix F and the overbars indicate averaging with respect to the ensemble of scatterers. If $\beta = 45^\circ$, (20) gives the correlation coefficient between the two orthogonal components of received signals in the circular basis. It is often referred to in the literature as ORTT. Setting $\beta = 0^\circ$ and 22.5° yields correlation coefficients in the linear and the proposed elliptical bases, respectively.

Figure 6 depicts this correlation coefficient de-

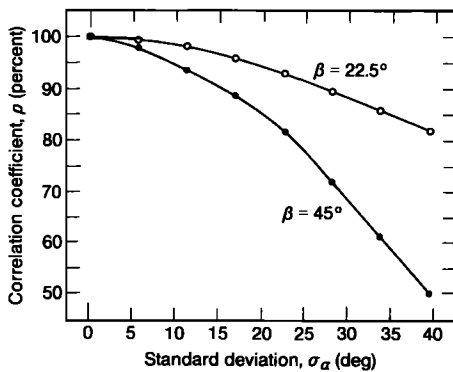


Fig. 6 Correlation coefficient between the two components of received signal amplitudes for circularly ($\beta = 45^\circ$) and elliptically ($\beta = 22.5^\circ$) polarized waves as a function of the standard deviation of the canting angle.

pendence on the standard deviation of the canting angle. It can be seen that the dynamic range of $\rho(45^\circ)$ is greater than that of $\rho(22.5^\circ)$. However, some approximate estimates of the particle degree of orientation can also be made in the case of elliptical polarization measurements. Correlation coefficients do not show strong dependence on the particle deformation (at least for the deformation values considered here) and on the mean canting angle, so data are presented for $A_0 = 2.2$ and $\alpha = 60^\circ$. However, for different values of A_0 and α , small percentage deviations from the data shown can be expected.

Errors in received power measurements also contribute to errors of the mean canting angle and the scattering amplitude retrieval and can sometimes make an exact solution of (16) impossible. In this case, applying the least squares procedure to solve this system of equations seems reasonable.

The particle mean canting angle α , which can be estimated by the proposed technique, characterizes scatterer orientation. If scatterers are observed at low elevations, α is close to the angle by which the particle symmetry axis deviates from the vertical. For cirrus clouds the most probable values of this angle are 0° for oblates and 90° for prolates. More dense clouds may show a large variety of particle preferable orientations in the vertical plane because of the influence of electric fields [McCormick and Hendry, 1979].

If scatterers are observed at high radar elevations, the mean canting angle shows the preferable particle orientation in the azimuthal plane. The

azimuthal distribution may be nonuniform because of, for example, wind shear or electrification. If we assume the homogeneity of horizontally extended cirrus clouds, estimations of the mean canting angle α at different elevations can provide general information about particle orientation with respect to horizontal and vertical planes.

As mentioned above, prolate and oblate scatterers cannot be distinguished from each other if measurements are made at a fixed elevation angle. However, some information about particle shapes can be obtained by analyzing the variations of depolarization ratio with the elevation angle. To do this, it is necessary to assume cloud homogeneity and small particle deviation from horizontal orientation. Model calculations show that for oblate scatterers with major axes that do not deviate from horizontal orientation by more than about 30° both depolarization ratios P_{cr}^a/P_{co}^a and P_{cr}^b/P_{co}^b as a rule tend to increase with increasing elevation angle. For prolate particles these ratios can have different tendencies depending on the particle azimuth orientation.

4. CONCLUSIONS

A method is proposed for estimating ice cloud particle axis ratios and the mean canting angle in the incident wave polarization plane. The method is based on an analysis of copolar and cross-polar components of received power. The use of elliptical polarization reduces differences between the two orthogonal components of received power. Such a technique may make it possible to analyze polarization components of radar echoes from low-reflectivity ice clouds, which may otherwise be too weak to detect in the orthogonal receiving channel when the usual linear or circular polarization measurements are made.

To separate shape and orientation effects, measurements can be made on two elliptical polarizations at polarization ellipse angles of 22.5° and -22.5° . As a result, a system of equations can be solved to estimate the mean canting angle and the scattering amplitudes ratio of scatterers in the incident wave polarization plane. The latter value can be converted into the scatterer minor-to-major dimension ratio if assumptions about the particle complex refractive index are made. Spread in the scatterer orientation causes errors in the estimated mean canting angles. This spread can be roughly

estimated by analyzing correlation coefficients between signal amplitudes in the two orthogonal receiving channels.

Acknowledgments. The author thanks R. A. Kropfli for productive discussions and helpful review of this paper. This work was done when the author held a National Research Associateship in the NOAA Wave Propagation Laboratory.

REFERENCES

- Atlas, D., M. Kerker, and W. Hitschfeld, Scattering and attenuation by non-spherical atmospheric particles, *J. Atmos. Terr. Phys.*, 3, 108–119, 1953.
- Bohren, C. F., and D. R. Huffman, *Absorption and Scattering of Light by Small Particles*, John Wiley, New York, 1983.
- Born, M., and E. Wolf, *Principles of Optics*, Pergamon, New York, 1965.
- Bringi, V. N., and A. Hendry, Technology of polarization diversity radars for meteorology, in *Radar in Meteorology*, edited by D. Atlas, pp. 153–190, American Meteorological Society, Boston, Mass., 1990.
- Holt, A. R., Some factors affecting the remote sensing of rain by polarization diversity radar in the 3- to 35- GHz frequency range, *Radio Sci.*, 19(5), 1399–1412, 1984.
- Kanareikin, D. B., S. Y. Matrosov, Y. A. Melnik, A. V. Ryzhkov, G. G. Schukin, A. B. Shupyatski, V. D. Stepanenko, and V. K. Zaviruha, Cloud and precipitation investigation by polarization diversity radars in the USSR, in *Program and Abstracts of the URSI Radio Science Meeting*, p. 368, Union Radio Scientifique Internationale, Paris, 1990.
- Kropfli, R. A., B. W. Bartram and S. Y. Matrosov, The upgraded WPL dual-polarization 8-mm wavelength Doppler radar for microphysical and climate research, in *Proceedings of the Conference on Cloud Physics*, pp. 341–345, American Meteorological Society, Boston, Mass., 1990.
- Magono, C., and C. W. Lee, Meteorological classification of natural snow crystals. *J. Fac. Sci. Hokkaido Univ., Ser. 7(4)*, 321–335, 1966.
- McCormick, G. C., and A. Hendry, Principles for the radar determination of the polarization properties of precipitation, *Radio Sci.*, 10(4), 421–434, 1975.
- McCormick, G. C., and A. Hendry, Radar measurement of precipitation-related depolarization in thunderstorms, *IEEE Trans. Geosci. Electron.*, GE-17(4), 142–150, 1979.
- McCormick, G. C., and A. Hendry, Optimal polarizations for partially polarized backscatter, *IEEE Trans. Antennas Propag.*, AP-33(1), 33–39, 1985.
- Melnik, Y. A., and A. V. Ryzhkov, Presentation of meteorological radar targets of different phase state on the Poincare sphere (in Russian), *Tr. Glavn. Geophys. Observ.*, 490, 17–21, 1985.
- Pruppacher, H. R., and J. D. Klett, *Microphysics of Clouds and Precipitation*, D. Reidel, Norwood, Mass., 1978.
- Rozenberg, V. I., *Scattering and Extinction of Electromagnetic Waves by Atmospheric Particles* (in Russian), Gidrometeoizdat, Leningrad, 1972.
- Van de Hulst, H. C., *Light Scattering by Small Particles*, Dover, New York, 1983.
- Yeh, C., R. Woo, A. Ishimaru, and J. Armstrong, Scattering by single ice needles and plates at 30 GHz, *Radio Sci.*, 17(6), 1503–1510, 1982.

S. Y. Matrosov, R/E/WP6, NOAA/Wave Propagation Laboratory, 325 Broadway, Boulder, CO 80303.